J Fluoresc (2013) 23:839–851
DOI 10.1007/s10895-013-1201-2

SHORT COMMUNICATION

A Combined Experimental and DFT-TDDFT Study of the Excited-State Intramolecular Proton Transfer (ESIPT) of 2-(2′-Hydroxyphenyl) Imidazole Derivatives

Vikas S. Padalkar · Ponnadurai Ramasami · Nagaiyan Sekar

Received: 19 November 2012 / Accepted: 24 February 2013 / Published online: 24 April 2013

Abstract We report a combined experimental and computational study of the effect of electron donor and acceptor groups on the excited state intramolecular proton transfer of 2-(2′-hydroxyphenyl) imidazole derivatives in solvents of different polarities. The changes in fluorescence properties, electronic transitions and energy levels are analyzed and discussed. The study was complemented using the Density Functional Theory (DFT)-Time Dependent DFT [B3LYP/6-31G(d)] computations. The calculated absorption and emission spectra of the imidazole derivatives are in good agreement with the experiments, thus allowing an assignment of the UV–vis spectra.

Keywords Benzimidazole · ESIPT · Fluorescence · Solvatochromism · DFT · TD DFT

Introduction

Excited state intramolecular proton transfer (ESIPT) is one of the proton transfer reactions that can be initiated by a light pulse. Proton transfer is the most important chemical reactions in chemistry and biology. The reaction dynamics and associated potential energy surfaces of the proton (hydrogen) transfer have been the subject of extensive investigation [1].

Excited-state intramolecular proton transfer (ESIPT) molecule shows large Stokes shift due to the characteristic four-level photophysical scheme incorporating the ground and excited states of two different tautomers. In the ground state, typical ESIPT molecules preferentially adopt enol (E) form, which is better stabilized by the intramolecular hydrogen-bonding. Upon photo-excitation, however, fast proton transfer reaction from the excited enol (E*) occurs to give the excited keto (K*) tautomer in a subpicosecond time scale. After decaying to the ground state, the keto (K) form reverts to the original enol form via reverse proton transfer. Different absorbing (E→E*) and emitting (K*→K) molecular species in this ESIPT cycle normally result in the total exclusion of self-absorption and the large Stokes' shifted keto emission [2–4]. A schematic diagram for ESIPT is shown in Scheme 1.

The ESIPT reaction generally incorporates transfer of a hydroxyl (or amino) proton to the carbonyl oxygen through a pre-existing hydrogen bonding configuration [5]. The resulting proton-transfer tautomer possesses significant differences in structure and electronic configuration from its corresponding normal species. The fundamental requirements of ESIPT process are the presence of intra-molecular hydrogen bonding between the acidic proton, basic moiety and the suitable geometry of molecular system. The acidic protons commonly involved are –OH and –NH_2 and basic centers are =N and –C=O [6–8]. Fluorescence due to ESIPT process is an effective tool in fluorescence based applications. ESIPT has attracted much more attention due to the wide applications in luminescent materials [9, 10], photopatterning [11], chemosensors [11], proton transfer laser [11], photostabilizers [12, 13], molecular logic gates

Electronic supplementary material The online version of this article (doi:10.1007/s10895-013-1201-2) contains supplementary material, which is available to authorized users.

V. S. Padalkar · N. Sekar (✉)
Tinctorial Chemistry Group,
Institute of Chemical Technology, Matunga,
Mumbai 400019, India
e-mail: n.sekar@ictmumbai.edu.in

V. S. Padalkar
e-mail: vikaspadalkar@gmail.com

P. Ramasami (✉)
Computational Chemistry Group, Department of Chemistry,
University of Mauritius, Réduit, Mauritius
e-mail: ramchemi@intnet.mu

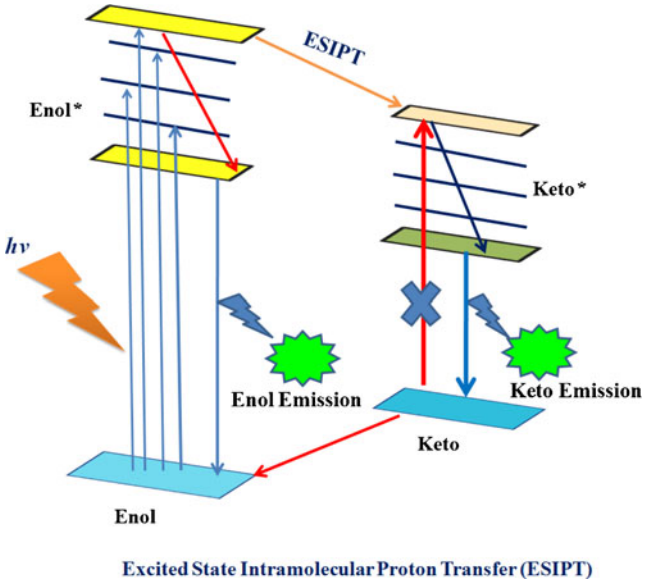

Scheme 1 ESIPT process

[14], molecular probes [15], metal ion sensors [16–18], radiation hard-scintillator counters [19, 20] and organic light emitting devices (OLEDs) [21]. ESIPT compounds have also drawn much attention due to their potential applications in optical devices [22] that may take advantage of the salient properties of the ESIPT compounds such as the ultra-fast reaction rate and extremely large fluorescence Stokes shift [23] compared to the normal fluorophores such as fluorescein, rhodamine or boron dipyrromethene (BODIPY) [23]. The large Stokes shift is a desired feature for fluorophores because the self-absorption, or the inner filter effect, can be avoided and the fluorescence analysis can be improved with this kind of fluorophores [24]. The nature of ESIPT has been well studied for a large number of organic molecules including some classic studies on methyl salicylate, salicylic acid and their derivatives [25, 26].

Among various ESIPT-active molecular structures, 2-(2′-hydroxyphenyl) benzoxazole (HBO) derivatives have been most often investigated due to their structural simplicity and facile chemical modification. 2-(2′-Hydroxyphenyl) benz oxazole (HBO) has emerged to be an interesting material, which exhibits a large Stokes shift (about 150 nm) arising from ESIPT [27–41].

This paper is a continuation of our interests on benzimidazole chemistry [42–44] to understand the effect of electron donor and electron acceptor on proton transfer process in the excited state, electronic transitions and energy levels in solvent of different polarities. We hereby report the changes in the electronic transition, energy levels, and orbital diagrams of previously synthesized HBO derivatives [42], Fig. 1. Compound **1** is simple benzimidazole, compound **2** contains the electron withdrawing NO_2 group and compound **3** contains the electron donating NH_2 group on imidazole core. This study was extended using the Density Functional Theory (DFT)-Time Dependent DFT [B3LYP/6-31G (d)] computations to shed more light on the absorption and emission spectra of compounds **1**–**3** at molecular level.

Methodology

Chemistry

2-(2′-Hydroxyphenyl) benzimidazole derivatives **1**–**3** were prepared according to previously published paper from our research group [42].

Computational Methods

The ground state geometry of the compounds **1**–**3** in their C_s symmetry were optimized using the tight criteria in the gas phase using DFT [45]. The functional used was B3LYP. The B3LYP method combines Becke's three parameter exchange functional (B3) [46] with the nonlocal correlation functional by Lee, Yang and Parr (LYP) [47]. The basis set used for all atoms was 6-31G(d) [48–50]. The vibrational frequencies of the optimized structures were computed using the same method to verify that the optimized structures correspond to local minima on the energy surface. The vertical excitation energies at the ground-state equilibrium geometries were calculated

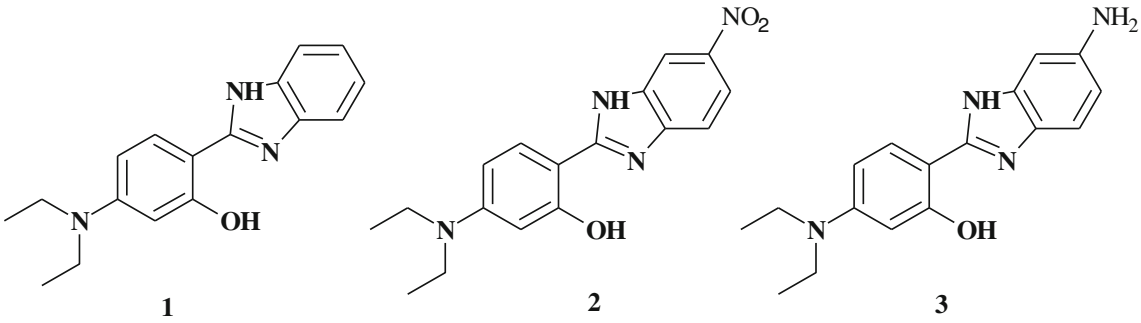

Fig. 1 2-(2′-hydroxyphenyl) benzimidazole derivatives, **1**–**3**

Table 1 Observed UV-visible absorption, computed absorption, observed emission and computed emission of compound **1** in different solvents

Solvent	TD DFT					[e]Assignment	Experimental emission			TD DFT (short emission) (nm)	Experimental long emission	[c]Stokes shift Δλ (nm)[c]	[d]Φ	%D
	λ_{max}^{Expt} (nm)	Vertical excitation		*f* (Oscillator)	%D		Observed emission (nm)	[a]Stokes shift Δλ (nm)	[b]Φ					
		nm	eV											
MeOH[f]	372	336	3.369	1.163	9.6	HOMO→LUMO (70 %)	393	21	0.11	384	518	146	0.03	2.2
EtOH	369	336	3.681	1.173	8.9	HOMO→LUMO (70 %)	400	31	0.10	383	–	–	–	4.2
ACN[f]	381	336	3.684	1.168	11.0	HOMO→LUMO (70 %)	394	13	0.13	384	486	105	0.02	2.5
DMF	360	336	3.684	1.173	6.6	HOMO→LUMO (70 %)	400	40	0.07	373	–	–	–	6.7
DCM	387	337	3.674	1.199	12.0	HOMO→LUMO (70 %)	403	16	0.10	376	–	–	–	6.6
$CHCl_3$[f]	390	337	3.676	1.195	13.0	HOMO→LUMO (70 %)	405	15	0.13	373	478	88	0.03	7.9
EtOAc	354	336	3.686	1.177	5.0	HOMO→LUMO (70 %)	388	34	0.12	376	–	–	–	3.0
Dioxane	354	336	3.690	1.188	5.0	HOMO→LUMO (70 %)	386	32	0.09	363	–	–	–	5.9
Acetone[f]	354	336	3.689	1.172	5.0	HOMO→LUMO (70 %)	402	48	0.11	383	486	132	0.02	4.7
DMSO[f]	363	337	3.669	1.191	7.1	HOMO→LUMO (70 %)	381	18	0.13	384	501	138	0.01	0.7

[a] Stokes shift for short emission

[b] Quantum yield at shorter wavelength

[c] Stokes shift for longer wavelength

[d] Quantum yield at longer wavelength

[e] Only major contributions are presented

[f] Dual emission

Analyses were carried out at room temperature (25 °C); experimentally observed λ_{max}

([%] D) % Deviation between vertical excitation and experimental absorption and experimental emission and computed (TD DFT) emission

MeOH Methanol, *EtOH* Ethanol, *ACN* Acetonitrile, *DMF* Dimethylformamide, *DCM* Dichloromethane, *$CHCl_3$* Chloroform, *EtOAc* Ethyl acetate, *DMSO* Dimethyl sulphoxide, *Dioxane* 1,4-Dioxane

Table 2 Observed UV-visible absorption, computed absorption, observed emission and computed emission of compound **2** in different solvents

Solvent	TD DFT				%D	[e]Assignment	Experimental emission			TD DFT (short emission) (nm)	Experimental emission			TD DFT (long emission) (nm)	%D
	λ_{max}^{Expt} (nm)	Vertical excitation		f (Oscillator)			Observed emission (nm)	[a]Stokes shift Δλ (nm)	[b]Φ		Observed emission (nm)	[c]Stokes shift Δλ (nm)	[d]Φ		
		nm	eV												
MeOH	333 393	342	3.619	1.085	12.0	HOMO→LUMO + 1 (69 %)	404	71	0.18	356	595	202	0.04	632	6.2
EtOH	333 399	342	3.616	1.085	14.0	HOMO→LUMO + 1 (69 %)	423	90	0.18	359	498	99	0.03	639	28.0
ACN	345 402	342	3.621	1.078	15.0	HOMO→LUMO + 1 (69 %)	430	85	0.20	360	530	128	0.01	642	21.0
DMF	336 405	343	3.607	1.109	15.0	HOMO→LUMO + 1 (69 %)	410	74	0.16	360	679	274	0.06	642	5.4
DCM	336 402	343	3.613	1.102	15.0	HOMO→LUMO + 1 (69 %)	424	88	0.19	356	635	233	0.01	625	1.5
$CHCl_3$	339 400	342	3.615	1.101	14.0	HOMO→LUMO + 1 (69 %)	412	73	0.19	352	610	210	0.009	607	0.5
EtOAc	324 405	342	3.624	1.084	15.0	HOMO→LUMO + 1 (69 %)	419	95	0.17	354	598	193	0.02	614	2.6
Dioxane	399	341	3.635	1.070	14.0	HOMO→LUMO + 1 (69 %)	–			344	531	111	0.20	537	1.1
Acetone	339 399	342	3.619	1.083	14.0	HOMO→LUMO + 1 (69 %)	454	115	0.19	360	638	239	0.03	638	0.0
DMSO	339 414	343	3.609	1.105	17.0	HOMO→LUMO + 1 (69 %)	402	115	0.19	360	510	224	0.03	644	26.0

[a] Stokes shift for short emission

[b] Quantum yield at shorter wavelength

[c] Stokes shift for longer wavelength

[d] Quantum yield at longer wavelength

[e] Only major contributions are presented

Analyses were carried out at room temperature (25 °C); experimentally observed λ_{max}

(%D) % Deviation between vertical excitation and experimental absorption and experimental emission and computed (TD DFT) emission

MeOH Methanol, *EtOH* Ethanol, *ACN* Acetonitrile, *DMF* Dimethylformamide, *DCM* Dichloromethane, *$CHCl_3$* Chloroform, *EtOAc* Ethyl acetate, *DMSO* Dimethyl sulphoxide, *Dioxane* 1,4-Dioxane

Table 3 Observed UV-visible absorption, computed absorption, observed emission and computed emission of compound **3** in different solvents

Solvent	TD DFT				%D	[e]Assignment	Experimental emission short			TD DFT (short emission) (nm)[c]	Experimental emission large			%D
	λ_{max}^{Expt} (nm)	Vertical excitation		*f* (Oscillator)			Observed emission (nm)	[a]Stokes shift Δλ (nm)	[b]Φ		Observed emission (nm)	[c]Stokes shift Δλ (nm)	[d]Φ	
		nm	eV											
MeOH	363	346	3.573	1.086	4.6	HOMO→LUMO (69 %)	436	73	0.12	411	–	–	–	5.7
EtOH	378	347	3.567	1.096	8.2	HOMO→LUMO (69 %)	441	68	0.12	411	–	–	–	6.8
ACN	375	347	3.570	1.092	7.4	HOMO→LUMO (69 %)	441	66	0.13	412	–	–	–	6.8
DMF	351	348	3.556	1.121	0.8	HOMO→LUMO (69 %)	436	85	0.10	412	–	–	–	5.5
DCM	354	348	3.560	1.111	1.6	HOMO→LUMO (69 %)	406	52	0.09	407	430	76	0.03	0.2
$CHCl_3$	369	348	3.561	1.110	5.6	HOMO→LUMO (69 %)	428	59	0.15	403	–	–	–	0.5
EtOAc	351	347	3.571	1.089	1.1	HOMO→LUMO (69 %)	429	78	0.11	405	441	90	0.02	5.5
Dioxane	354	347	3.572	1.088	1.9	HOMO→LUMO (69 %)	431	77	0.09	409	–	–	–	5.1
Acetone	366	347	3.568	1.095	5.1	HOMO→LUMO (69 %)	440	74	0.12	411	–	–	–	6.5
DMSO	375	348	3.557	1.117	7.2	HOMO→LUMO (69 %)	446	71	0.13	412	–	–	–	7.6

[a] Stokes shift for short emission

[b] Quantum yield at shorter wavelength

[c] Stokes shift for longer wavelength

[d] Quantum yield at longer wavelength

[e] Only major contributions are presented

Analyses were carried out at room temperature (25 °C); experimentally observed λ_{max}

(%D) % Deviation between vertical excitation and experimental absorption and experimental emission and computed (TD DFT) emission

MeOH Methanol, *EtOH* Ethanol, *ACN* Acetonitrile, *DMF* Dimethylformamide, *DCM* Dichloromethane, *$CHCl_3$* Chloroform, *EtOAc* Ethyl acetate, *DMSO* Dimethyl sulphoxide, *Dioxane* 1,4-Dioxane

with TD DFT [51]. The low-lying first singlet excited state (S_1) of each conformer was relaxed using the TD DFT to obtain its minimum energy geometry. The difference between the energies of the optimized geometries at the first singlet excited state and the ground state was used in computing the emissions [52, 53]. Frequency computations were also carried out on Frank-Condon excited state of conformers. All the computations in solvents of different polarities were carried out using the Polarizable Continuum Model (PCM) [54, 55]. All electronic structure computations were carried out using the Gaussian 09 program [56].

Relative Quantum Yield Calculations

Quantum yields of the synthesized compounds in different solvents were calculated by using anthracene as the reference standard in different solvents using the comparative method [57, 58]. Absorption and emission spectra of the standard and the compounds in polar as well as non-polar solvents were measured at different concentrations at (2, 4, 6, 8, and 10 ppm level). Emission intensity values were plotted against absorbance values and linear plots were obtained. Gradients were calculated for compounds in each solvent and for the standards. All the measurements were done by keeping parameters such as solvent and slit width constant. Relative quantum yields of synthesized compounds in different solvents were calculated by using Eq. 1 [57, 58].

$$\Phi_X = \Phi_{St}\left(\frac{Grad_X}{Grad_{St}}\right)\left(\frac{\eta_X^2}{\eta_{St}^2}\right) \quad (1)$$

Where:

Φ_X	Quantum yield of synthesized compound
Φ_{St}	Quantum yield of standard sample
$Grad_X$	Gradient of synthesized compound
$Grad_{St}$	Gradient of standard sample
η_X	Refractive index of solvent used for synthesized compound
η_{St}	Refractive index of solvent used for standard sample

Result and Discussion

Photophysical Properties

Compounds **1**–**3** are fluorescent in solution on irradiation with UV light. The effects of solvent polarities on absorption and emission properties of the compounds are summarized in Tables 1, 2 and 3. Compound **1** is sensitive towards the polarity of solvents but the trend is not regular from non-polar to polar solvent or vice-versa. Experimentally, the observed absorption wavelength in different solvents ranges from 354 to 390 nm and the computed vertical excitation in all solvents are about 336 nm. The observed difference in ethyl acetate, di oxane and acetone is 18 nm which is the lowest and the largest difference is 53 nm in chloroform. The % deviation between theoretical and experimental absorption (compound **1** absorption range 354–381 nm and vertical excitation 336–337 nm; compound **2** absorption range 333–414 and vertical excitation 341–343; compound **3** absorption range 354–378 and vertical excitation 346–348) ranges from 5 to 13 %. In ethyl acetate, di oxane and acetone, the % deviation is 5 %, while in chloroform and dichloromethane,

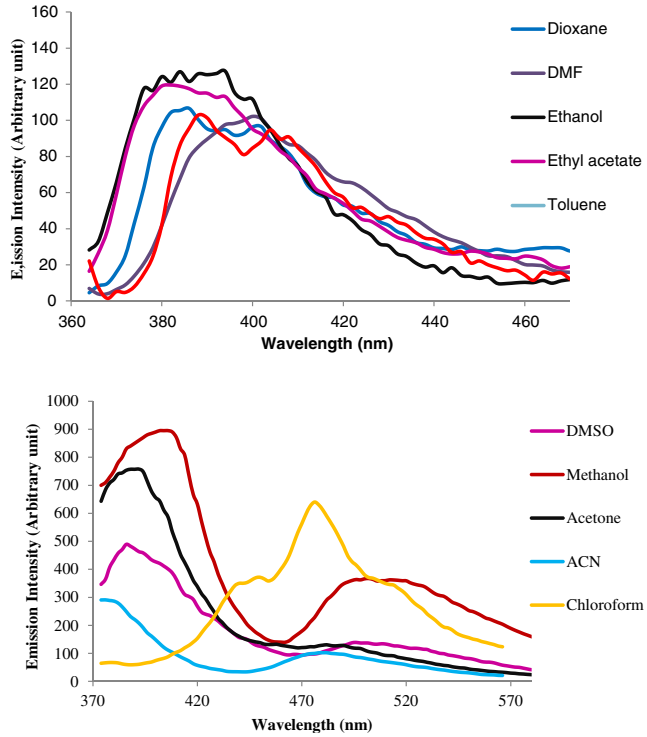

Fig. 2 Emission spectra of compound **1** in different solvents

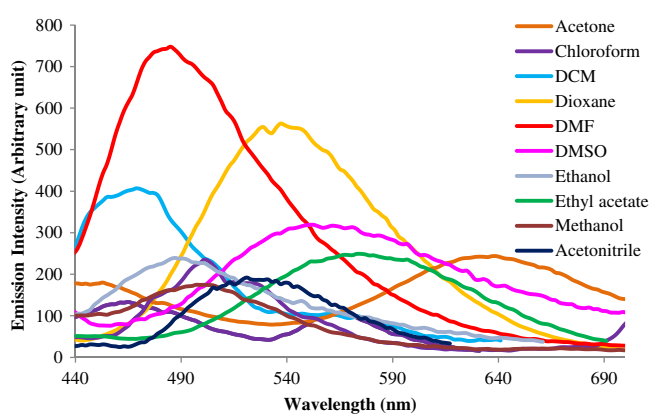

Fig. 3 Emission spectra of compound **2** in different solvents

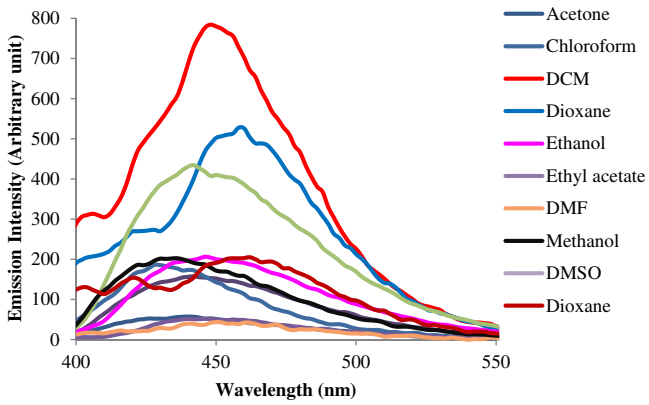

Fig. 4 Emission spectra of compound **3** in different solvents

the % deviation is 13 %. In all the solvents, excitation is from HOMO to LUMO orbital. Observed absorption, molar absorptivity and computed vertical excitations of compound **1** are summarized in Table 1.

The solvatofluorism study reveals that compound **1** showed single emission in some solvents (dioxane, DMF, ethanol, ethyl acetate, toluene) while in DMSO, methanol, acetone and acetonitrile the compound shows dual emission with an intense emission peak found between 370 and 420 nm and there is a shoulder peak is between 470 and 570 nm. In case of chloroform as the solvent, a shoulder peak is observed at 460 nm with additional intense peak being observed at 475 nm. It is well known that the long wavelength emission in ESIPT compounds is attributed to the excited state keto tautomer originating from the excited state enol tautomer [34]. The driving force behind the proton transfer is the associated intrinsic extra stabilization of the keto tautomer at the excited state.

Quantum yield is sensitive to the solvent polarities. It is observed that the quantum yield is higher in DMSO, ethyl acetate and methanol than in DMF, dioxane and acetonitrile. This can be attributed to the contribution coming from the long wavelength emission. The quantum efficiency was much higher in DMF and acetonitrile (Φ=0.13) than the other polar solvents. The short wavelength emission occurs in all cases with a narrow range of Stokes shift (15–48 nm). It is interesting to note that the short wavelength emission is much red shifted in DCM and acetone (Fig. 2 and Table 1). Solvent polarities also affect the Stokes shift for longer emission and ranges from 88 to 146 nm.

Table 4 Frontier molecular orbital's of fluorophores **1**–**3** in acetone with their energy

Compound	HOMO	LUMO
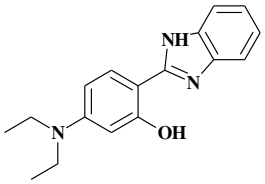	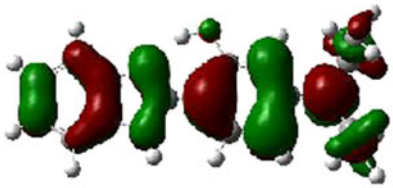	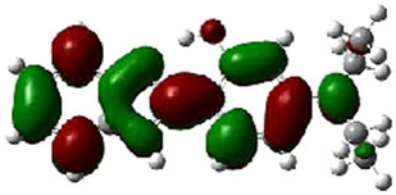
1	**-0.3144 eV**	**-0.2099 eV**
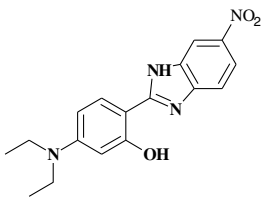	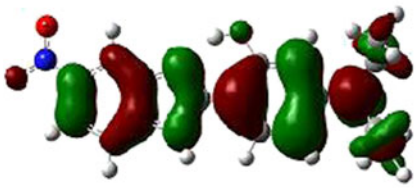	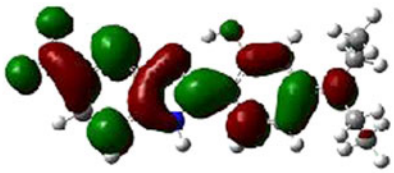
2	**-0.3140 eV**	**-0.2139 eV**
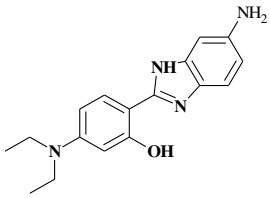	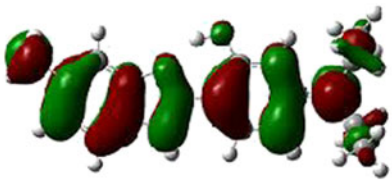	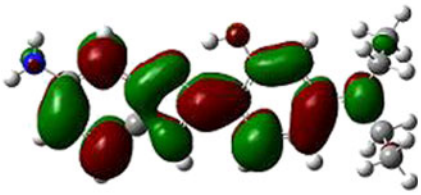
3	**-0.3095 eV**	**-0.2084 eV**

Table 5 Structural properties of compound **1**

Properties	**1** (Enol)		**1** (Keto)	
Stoichiometry	$C_{17}H_{19}N_3O$		$C_{17}H_{19}N_3O$	
Framework group	$C_1(\times(C_{17}H_{19}N_3O)$		$C_1(\times(C_{17}H_{19}N_3O)$	
				
Bond distance	Bond	Bond Length	Bond	Bond Length
	$r(C_1\text{-}O_{24})$	1.352	$r(C_1\text{-}O_{24})$	1.203
	$r(C_{12}\text{-}N_{23})$	1.332	$r(C_{12}\text{-}N_{23})$	1.356
	$r(C_{12}\text{-}C_2)$	1.448	$r(C_{12}\text{-}C_2)$	1.415
Bond angle	Angle	Bond Angle	Angle	Bond Angle
	$A(N_{23}\text{-}C_{12}\text{-}C_2)$	123.7	$A(N_{23}\text{-}C_{12}\text{-}C_2)$	123.1
	$A(C_{12}\text{-}C_2\text{-}C_1)$	120.0	$A(C_{12}\text{-}C_2\text{-}C_1)$	118.4
	$A(C_2\text{-}C_1\text{-}O_{24})$	122.1	$A(C_2\text{-}C_1\text{-}O_{24})$	122.4
Dihedral angle	$A(N_{23}\text{-}C_{12}\text{-}C_2\text{-}C_1)$	0.025	$A(N_{23}\text{-}C_{12}\text{-}C_2\text{-}C_1)$	0.004

Bond angle in °, Bond length in Å

Compound **2** contains the strong electron withdrawing –NO_2 group which enhances the ESIPT process by increasing the electron density on N in imidazole and the acidity of hydroxy H. Compound **2** is also sensitive towards the solvent polarity. In all the solvents compound **2** shows dual absorption, first absorption around 333 nm and longer emission around 400 nm. A large difference of 18 nm is observed between experimental absorption and vertical excitation in ethyl acetate. Compound **2** does not show solvatochromism; in DMSO it shows red shift as compared to other solvents. Compound **2** shows solvatofluorism properties from 402 nm

Table 6 Structural properties of compound **2**

Properties	**2** (Enol)		**2** (Keto)	
Stoichiometry	$C_{17}H_{18}N_4O_3$		$C_{17}H_{18}N_4O_3$	
Framework group	$C_1(\times(C_{17}H_{18}N_4O_3)$		$C_1(\times(C_{17}H_{18}N_4O_3)$	
	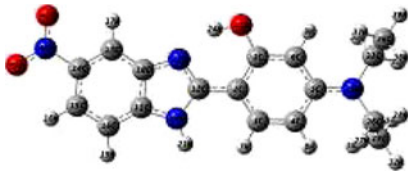		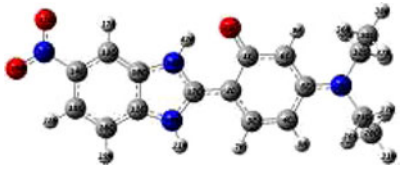	
Bond distance	Bond	Bond Length	Bond	Bond Length
	$r(C_1\text{-}O_{23})$	1.351	$r(C_1\text{-}O_{23})$	1.281
	$r(C_{12}\text{-}N_{22})$	1.333	$r(C_{12}\text{-}N_{22})$	1.358
	$r(C_{12}\text{-}C_2)$	1.412	$r(C_{12}\text{-}C_2)$	1.406
Bond angle	Angle	Bond Angle	Angle	Bond Angle
	$A(N_{22}\text{-}C_{12}\text{-}C_2)$	123.7	$A(N_{22}\text{-}C_{12}\text{-}C_2)$	123.3
	$A(C_{12}\text{-}C_2\text{-}C_1)$	120.0	$A(C_{12}\text{-}C_2\text{-}C_1)$	118.2
	$A(C_2\text{-}C_1\text{-}O_{23})$	122.0	$A(C_2\text{-}C_1\text{-}O_{23})$	122.2
Dihedral angle	$A(N_{22}\text{-}C_{12}\text{-}C_2\text{-}C_1)$	0.68	$A(N_{22}\text{-}C_{12}\text{-}C_2\text{-}C_1)$	0.25

Bond angle in °, Bond length in Å

Table 7 Structural properties of compound **3**

Properties	**3** (Enol)		**3** (Keto)	
Stoichiometry	$C_{17}H_{20}N_4O$		$C_{17}H_{20}N_4O$	
Framework group	$C_1(\times(C_{17}H_{20}N_4O)$		$C_1(\times(C_{17}H_{20}N_4O)$	
	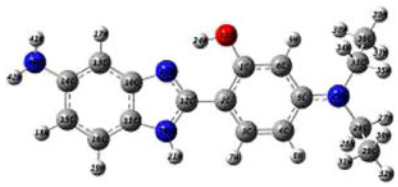		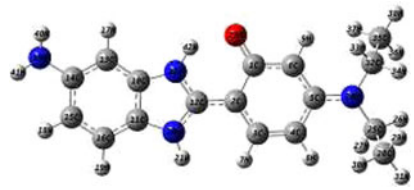	
Bond distance	Bond	Bond length	Bond	Bond length
	$r(C_1\text{-}O_{23})$	1.352	$r(C_1\text{-}O_{23})$	1.284
	$r(C_{12}\text{-}N_{22})$	1.336	$r(C_{12}\text{-}N_{22})$	1.357
	$r(C_{12}\text{-}C_2)$	1.449	$r(C_{12}\text{-}C_2)$	1.418
Bond angle	Angle	Bond Angle	Angle	Bond Angle
	$A(N_{22}\text{-}C_{12}\text{-}C_2)$	123.4	$A(N_{10}\text{-}C_9\text{-}C_5)$	123.0
	$A(C_{12}\text{-}C_2\text{-}C_1)$	119.0	$A(C_4\text{-}C_5\text{-}C_9)$	118.5
	$A(C_2\text{-}C_1\text{-}O_{23})$	122.0	$A(O_7\text{-}C_4\text{-}C_5)$	122.5
Dihedral angle	$A(N_{22}\text{-}C_{12}\text{-}C_2\text{-}C_1)$	0.74	$A(N_{10}\text{-}C_9\text{-}C_5\text{-}C_4)$	0.30

Bond angle in ^{o}, Bond length in Å

to 452 nm. It shows dual emission in all solvents except in dioxane; short emission is between 402 and 430 nm and longer emission is located between 537 and 644 nm. Observed stokes shift due to longer emission (99–274 nm) is larger as compared to Stokes shift due to short emission (71–115 nm). Emission spectra are shown in Fig. 3. Observed absorption, vertical excitation, experimental emission, emission by TD DFT and quantum yield of compound **2** are summarized in Table 2.

Compound **3** contain the electron releasing $–NH_2$ group on the benzimidazole ring. Observed absorption, vertical excitation, emission and quantum yield are summarized in Table 3 and emission spectra are shown in Fig. 4. Compound **3** shows red shift in ethanol, acetonitrile and dimethyl sulphoxide. The difference between experimental absorption and vertical excitation is 4 nm in ethyl acetate and DMF. A large difference between vertical excitation and experimental emission was observed in ethanol, acetonitrile and dimethyl sulphoxide. The % deviation between experimental and theoretical absorption is in the range 0.8–8.2 %. Compound **3** shows dual emission in dichloromethane and ethyl acetate and single emission in other solvents. Stokes shift due to short emission as well as long emission is almost same. The quantum yield of compound **3** varies from 0.09 to 0.13.

Compound **2** shows red shift as compared to compounds **1** and **3**. Compound **2** contains the NO_2 group para to the

Table 8 Dipole moment (μ in Debye) of compound **1** in ground state and excited state in various solvents

Medium	E_T^N	Compound **1** [a]Enol μ_g	Compound **1** [b]Enol μ_e	$\frac{\mu_e Enol}{\mu_g Enol}$	Compound **1** [a]Keto μ_g	Compound **1** [b]Keto μ_e	$\frac{\mu_e Keto}{\mu_g Keto}$	Experimental $\frac{\mu_e Enol}{\mu_g Enol}$
MeOH	0.775	4.826	7.421	1.537	6.594	6.978	1.058	1.3373 At short emission (enol form) 2.3703 for long emission (enol form)
EtOH	0.654	4.824	7.374	1.528	6.550	6.980	1.065	
ACN	0.460	4.827	7.434	1.540	6.606	6.987	1.057	
DMF	0.386	4.827	6.789	1.406	6.612	6.990	1.057	
DMSO	0.396	4.828	7.467	1.546	6.638	7.008	1.055	
DCM	0.309	4.807	9.654	2.008	6.248	6.715	1.074	
$CHCl_3$	0.259	4.787	6.664	1.321	5.893	6.080	1.031	
EtOAc	0.228	4.496	6.830	1.519	6.044	6.554	1.084	
Acetone	0.207	4.822	7.333	1.520	6.511	6.920	1.062	
Dioxane	0.164	4.747	5.955	1.254	5.260	6.654	1.265	

[a]Dipole moments were obtained at the optimized ground state geometry; [b]Dipole moments were obtained at the optimized excited state geometry

Table 9 Dipole moment (μ in Debye) of compound **2** in the ground and excited state in various solvents

Medium	E_T^N	Compound **2** [a]Enol μ_g	Compound **2** [b]Enol μ_e	$\frac{\mu_e Enol}{\mu_g Enol}$	Compound **2** [a]Keto μ_g	Compound **2** [b]Keto μ_e	$\frac{\mu_e Keto}{\mu_g Keto}$	Experimental $\frac{\mu_e Enol}{\mu_g Enol}$
MeOH	0.775	10.937	11.263	1.029	11.613	11.263	0.969	2.3369 for short emission (enol form)
EtOH	0.654	14.005	14.916	1.065	11.563	11.209	0.969	
ACN	0.460	14.083	15.017	1.066	11.629	11.280	0.969	
DMF	0.386	10.748	15.027	1.397	11.635	11.312	0.972	
DMSO	0.396	14.126	15.075	1.071	11.666	11.323	0.970	
DCM	0.309	10.891	14.351	1.317	11.204	10.778	0.961	2.3395 for long emission (enol form)
$CHCl_3$	0.259	10.843	13.672	1.260	10.773	10.263	0.952	
EtOAc	0.228	10.868	13.965	1.284	10.959	10.486	0.956	
Acetone	0.207	10.925	14.844	1.359	11.517	11.151	0.968	
Dioxane	0.164	10.788	12.400	1.149	9.970	9.308	0.933	

[a]Dipole moments were obtained at the optimized ground state geometry; [b]Dipole moments were obtained at the optimized excited state geometry

substituted *N,N*-diethylamino and hydroxyl electron donor unit. The NO_2 group increases the acidity of hydrogen and basicity of N of imidazole core which causes enhancement of ESIPT and, a red shift is observed for absorption as well as emission. In case of compound **3**, electron donor NH_2 group present on electron withdrawing unit decreases the basicity of imidazole N and acidity of hydroxyl H and affects the ESIPT process of compound **3** leading to single emission in most of solvent.

Frontier molecular orbitals and their energies were obtained and HOMO and LUMO orbital diagrams are shown in Table 4 for compounds **1**–**3** in acetone solvent. The compounds contain electron donor and acceptor system, the substituted benzimidazole unit acts as an electron acceptor and the *N,N*-diethyl and hydroxy substituted benzene unit act as electron donor. In the case of HOMO, the electron density is distributed across the compounds **1**–**3**, while in the LUMO, the electron density is localized along the benzimidazole unit of compounds **1**–**3**, it shows nodes on *N,N*-diethyl group. The HOMO-LUMO energy gap for compound **2** (0.1001 eV) is less as compared to compound **1** (0.1053 eV) and **3** (0.1011 eV) due to the effective charge transfer from electron donor to acceptor for compound **1** which has NO_2 as an efficient electron acceptor and enhances the ESIPT process. This is reflected in the red shift of absorption as well as emission, see Tables 1, 2 and 3. The HOMO-LUMO orbital diagrams of compound **1** in all solvents for the enol form as well as the keto form show similar electron distribution pattern Tables 11–12 (Supporting Information). Computed vertical excitation and emission of compounds **1**–**3** for keto form are summarized in Tables 13–15 (Supporting Information).

Structural Properties of Compounds **1**–**3**

The structural changes due to ESIPT phenomenon in terms of bond angle, bond distance and geometry of the electron donor and acceptor groups are investigated by using optimized geometries as shown in Tables 5, 6 and 7. Results of bond angle and bond length clearly indicate that, due to the intra-molecular hydrogen bonding the compounds has a six-member ring conformation in excited state. The main feature of the molecular structures like stiochiometry, framework group, degree of freedom and point group of compounds remain the same in both enol and keto forms which can be deduced from Tables 5, 6 and 7 for all the compounds 1–3. In compound **1**, the bond length [r_{Enol} (C_1-O_{24}); 1.352 Å] and [r_{Keto} (C_1-O_{24}); 1.203 Å] and bond angle [r_{Enol} (C_2-C_1-O_{24}); 122.1 Å

Table 10 Dipole moment (μ in Debye) of compound **3** in the ground and excited state in various solvents

Medium	E_T^N	Compound **3** [a]Enol μ_g	Compound **3** [b]Enol μ_e	$\frac{\mu_e Enol}{\mu_g Enol}$	Compound **3** [a]Keto μ_g	Compound **3** [b]Keto μ_e	$\frac{\mu_e Keto}{\mu_g Keto}$	Experimental $\frac{\mu_e Enol}{\mu_g Enol}$
MeOH	0.775	3.927	5.283	1.345	6.782	7.058	1.040	2.020 at short emission (enol form) 1.8421 for long emission (enol form)
EtOH	0.654	3.924	5.240	1.335	6.782	7.058	1.040	
ACN	0.460	3.928	5.295	1.348	6.794	6.990	1.208	
DMF	0.386	3.928	5.300	1.349	6.697	7.060	1.054	
DMSO	0.396	3.930	5.325	1.569	6.225	7.060	1.134	
DCM	0.309	3.904	4.948	1.267	6.432	7.070	1.099	
$CHCl_3$	0.259	3.880	4.599	1.185	6.070	6.960	1.146	
EtOAc	0.228	3.890	4.749	1.220	6.782	7.013	1.034	
Acetone	0.207	3.922	5.202	1.326	6.699	7.054	1.052	
Dioxane	0.164	3.834	6.497	1.694	5.416	6.497	1.199	

[a]Dipole moments were obtained at the optimized ground state geometry; [b]Dipole moments were obtained at the optimized excited state geometry

and A_{keto} A(C_2-C_1-O_{24});122.4 Å] differ from each other in the enol and keto forms respectively. The change in bond length clearly indicates that ESIPT phenomenon is observed in compound **1**. Similar trends are observed for compounds **2** and **3**. Compounds **1**–**3** are roughly planar in enol and keto forms and, this facilitates the excited state intra-molecular hydrogen transfer. The hydroxyl group is para to imidazole, oxazole and thiazole and it increases the basicity of nitrogen present in the ring. This is further confirmed by our computations. In enol form, the lone pair of electrons present on oxygen is involved in resonance, the single bond length character is converted in to double bond character hence the bond length between O-H decreases as compared to keto form. This is also observed for other compounds. The changes in bond length, bond angle and dihedral angle due to excited state intramolecular phenomenon for all compounds are summarized in Tables 5, 6 and 7.

Effect of Solvent Polarity on Ground and Excited State Dipole Moments

Dipole moments of compounds **1**–**3** in the ground state and excited stated were computed for short as well as long emission in solvents of different polarities. The ratio of dipole moment in excited to ground state in different solvents is plotted against the solvent function (E_T^N) (Tables 8, 9 and 10, Figs. 5 and 6). The solvent polarity function has been taken from the literature [59]. The experimental dipole moment ratio for compound **1** is 1.337 and is 2.370 for longer emission. Compound **2** shows highest dipole moment in all solvents as compared to compounds **1** and **3** experimentally as well theoretically. The dipole moment of compound **1** ranges from 4.2 D to 4.8 D for enol form and 6.6 to 9.6 D for the excited state. Dipole moment of compounds **1**–**3** are almost same in different solvents for each compound which accounts for almost similar absorption properties of compounds.

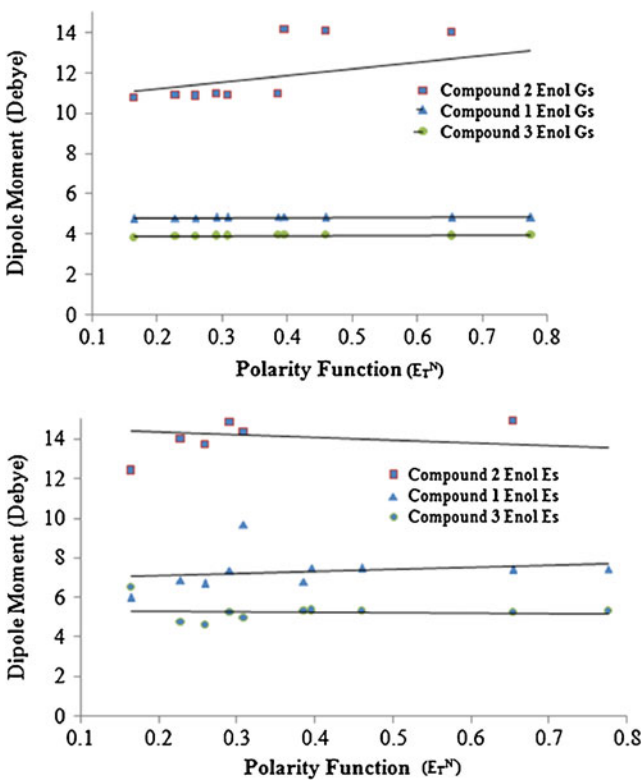

Fig. 5 Plots of dipole moment (μ) versus solvent polarity function (E_N^T) of compounds **1**–**3** enol form in the ground and excited state

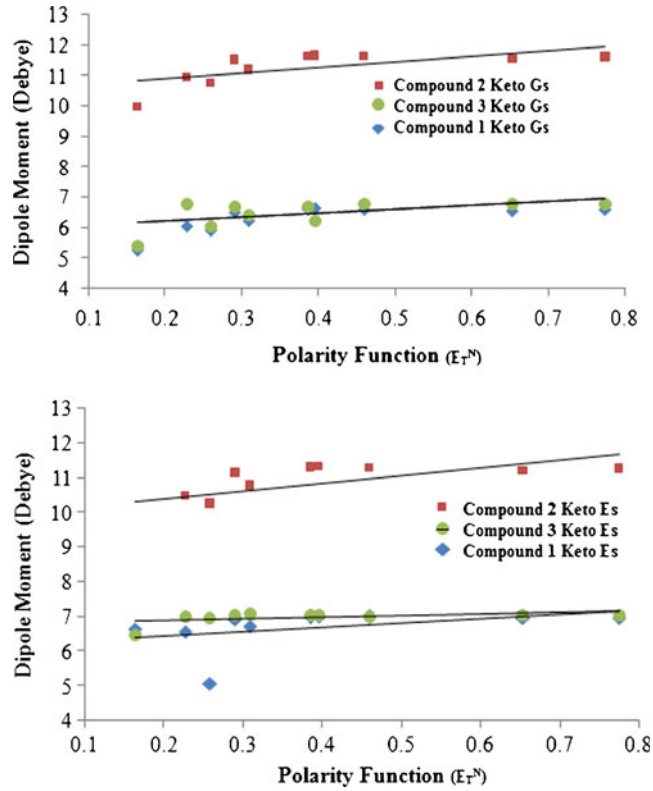

Fig. 6 Plots of dipole moment (μ) versus solvent polarity function (E_N^T) of compounds **1**–**3** keto form in the ground and excited state

Conclusion

Photo-physical properties of 2-(2′-hydroxyphenyl) imidazole derivatives were studied in solvents of different polarities. The absorption and emission wavelengths were computed using TD DFT and they are in good agreement with the experimental results, the HOMO-LUMO gap for each compound is the same in all the solvents. Compound **1** shows dual emission, intense peak at short wavelength and shoulder peak at longer wavelength in DMSO, methanol, acetone and acetonitrile. In case of chloroform shoulder peak at short wavelength and intense peak at long wavelength was observed. Compound **2** shows dual emission in all the solvents studied except for

dioxane, and compound **3** shows dual emission in DCM and ethyl acetate only. The compounds show large Stokes shift due to ESIPT process and this can be important as fluorescence compounds with large Stokes shift are used as fluorescence probes. The computational methods have been useful for assignments of the absorption and emission and thus lead to more understanding at molecular level and this is not possible by experiments alone. We hope that our research will be helpful to future uses of these compounds as they show very good fluorescence properties.

References

1. Valeur B (2001) Molecular fluorescence: principles and applications. Wiley-VCH, Verlag GmbH, ch 4, pp 99–106
2. Seo J, Kim S, Park S, Park SY (2005) Tailoring the excited-state intramolecular proton transfer (ESIPT) fluorescence of 2-(2′-hydroxyphenyl) benzoxazole derivatives. Bull Korean Chem Soc 26:1706–1710
3. Lochbrunner S, Wurzer AJ, Riedle E (2000) Ultrafast excited-state proton transfer and subsequent coherent skeletal motion of 2-(2′-hydroxyphenyl)benzothiazole. J Chem Phys 112:10699–10702
4. Takeuchi S, Tahara TJ (2005) Coherent excited state intramolecular proton transfer probed by time-resolved fluorescence. J Phys Chem A 109:10199–10207
5. Sinha H, Dogra S (1986) Ground and excited state prototropic reactions in 2-(*o*-hydroxyphenyl) benzimidazole. Chem Phys 102:337–347
6. Das K, Mjumder D, Bhattacharyya K (1992) Excited-state intramolecular proton transfer in 2-(2′, 6′-dihydroxyphenyl) benzoxazole: effect of dual hydrogen bonding on the optical properties. Chem Phys Lett 198:443–448
7. Douhal A, Amat-Guerri F, Lillo M, Acuna A (1994) Proton transfer spectroscopy of 2-(2′-hydroxyphenyl) imidazole and 2-(2′-hydroxyphenyl) benzimidazole dyes. J Photochem Photobiol A Chem 78:127–138
8. Rios M (1995) Thermodynamics of micelle formation of chlorhexidine digluconate. J Phys Chem 99:17628–17631
9. Kwon JE, Park SY (2011) Advanced organic optoelectronic materials: harnessing Excited-State Intramolecular Proton Transfer (ESIPT). Process Adv Mater 23:3615–3642
10. Tang KC, Chang MJ, Lin TY, Pan HA, Fang TC, Chen KY, Hung WY, Hsu YH, Chou PT (2011) Fine tuning the energetic of excited-state intramolecular proton transfer (ESIPT): white light generation in a single ESIPT system. J Am Chem Soc 133:17738–17745
11. Chen KY, Hsieh CC, Cheng YM, Lai CH, Chou PT (2006) Extensive spectral tuning of the proton transfer emission from 550 to 675 nm via a rational derivatization of 10-hydroxybenzo [h] quinoline. Chem Commun:4395–4397
12. Stuber GJ, Kieninger M, Schettler H, Busch W, Goller B, Frnke J, Kramer HEA, Hoier H, Henkel S, Fischer P, Port H, Hirsch T, Rytz G, Birbaum J-L (1995) Ultraviolet stabilizers of the 2-(2′-hydroxyphenyl)-1, 3, 5-triazine class: structural and spectroscopic characterization. J Phys Chem 99:10097–10109
13. Keck J, Kramer HEA, Port H, Hirsch T, Fischer P, Rytz G (1996) Investigations on polymeric and monomeric intra-molecularly hydrogen-bridged UV absorbers of the benzotriazole and triazine class. J Phys Chem 100:14468–14475
14. Luxami V, Kumar S (2008) Molecular half-subtractor based on 3, 3′-bis (1H-benzimidazolyl-2-yl)[1, 1′] binaphthalenyl-2, 2′-diol. New J Chem 32:2074–2079
15. Wu JS, Liu WM, Ge JC, Zhang HY, Wang PF (2011) New sensing mechanisms for design of fluorescent chemosensors emerging in recent years. Chem Soc Rev 40:3483–3495
16. Taki M, Wolford JL, O'Halloran TV (2004) Emission ratiometric imaging of intracellular zinc: design of a benzoxazole fluorescent sensor and its application in two-photon microscopy. J Am Chem Soc 126:712–713
17. Ohshima A, Momotake A, Arai T (2004) Chemistry of aminophenols. Part 3: first synthesis of nitrobenzo[*b*]furans via a coupling–cyclization approach. Tetrahedron Lett 45:9377–9380
18. Rodembusch FS, Brand FR, Correa DS, Pocos JC, Martinelli M, Stefani V (2005) Transition metal complexes from 2-(2′-hydroxyphenyl) benzoxazole: a spectroscopic and thermogravimetric stability study. Mater Chem Phys 92:389–396
19. Pla-Dalmau A (1995) 2-(2′-hydroxyphenyl) benzothiazoles, -benzoxazoles, and -benzimidazoles for plastic scintillation applications. J Org Chem 60:5468–5473
20. Pla-Dalmau A, Foster GW, Zhang G (1996) Gamma-irradiation of coumarins in a polystyrene matrix. Radiat Phys Chem 148:519–524
21. Vazquez SR, Rodriguez MCR, Mosquera M, Rodriguez Prieto F (2007) Advances in radiological image analysis. J Phys Chem A 111:1814–1818
22. Zhang G, Wang H, Yu Y, Xiong F, Tang G, Chen W (2003) Optical switching of 2-(2′-hydroxyphenyl) benzoxazole in different solvents. Appl Phys B Lasers Opt 76:677–681
23. Xu Y, Pang Y (2011) Zn^{2+}triggered excited-state intramolecular proton transfer: a sensitive probe with near-infrared emission from bis(benzoxazole)derivative. Dalton Trans 40:1503–1509
24. Zhao J, Ji S, Chen Y, Guo H, Yang P (2012) Excited state intramolecular proton transfer (ESIPT): from principal photophysics to the development of new chromophores and applications in fluorescent molecular probes and luminescent materials. Phys Chem Chem Phys 14:8803–8817
25. McCarthy A, Ruth A (2011) Fluorescence excitation and excited state intramolecular proton transfer of jet-cooled naphthol derivatives: part 2. 2-hydroxy-1-naphthaldehyde. Phys Chem Chem Phys 13:18661–18670
26. Andrzej L, Wolfgang D (1999) Ab initio potential-energy functions for excited state intramolecular proton transfer: a comparative study of *o*-hydroxybenzaldehyde, salicylic acid and 7-hydroxy-1-indanone. Phys Chem Chem Phys 1:3065–3072
27. Kelly R, Schulman S, Schulman S (1988) Molecular luminisons spectroscopy, methods and applications part -2. Wiley Interscience, New York, Chapter 6
28. Ghiggino K, Scully A, Leaver I (1986) Effect of solvent on excited-state intramolecular proton transfer in benzotriazole photostabilizers. J Phys Chem 90:5089–5093
29. Kosower E, Huppert D (1986) Excited state electron and proton transfers. Annu Rev Phys Chem 37:127–156
30. Law K, Shoham J (1995) Photoinduced proton transfers in 3,5-di-tert-butylsalicylic acid. J Phys Chem 99:12103–12108
31. Goodman J, Brus L (1978) Proton transfer and tautomerism in an excited state of methyl salicylate. J Am Chem Soc 100:7472–7474
32. Herek J, Pedersen S, Banares L, Zewali A (1992) Femtosecond real-time probing of reactions. IX. Hydrogen-atom transfer. J Chem Phys 97:9046–9061
33. Formosinho S, Arnaut J (1993) Electrically generated intramolecular proton transfer: electroluminescence and stimulated emission from polymers. J Photochem Photobiol A Chem 75:21–48
34. Segala M, Dorirngues N, Livotto V, Stefani V (1999) Heterocyclic dyes displaying Excited-State Intramolecular Proton-Transfer reactions (ESIPT): computational study of the substitution effect on the electronic absorption spectra of 2-(2′-hydroxyphenyl)benzoxazole derivatives. J Chem Soc Perkin Trans 2 2:1123–1128
35. Elguero J, Katritzky AR, Denisko O (2000) Prototropic tautomerism of heterocycles: heteroaromatic tautomerism–general overview and methodology. Adv Heterocycl Chem 76:1–84

36. Arnaut L, Formosinho S (1993) Excited-state proton transfer reactions. Fundamentals and intermolecular reactions. J Photochem Photobiol A Chem 75:1–20
37. Formosinho S, Arnaut L (1993) Excited-state proton transfer reactions II. Intramolecular reactions. J Photochem Photobiol A Chem 75:21–48
38. Rios N, Rios M (1998) Ab initio study of the hydrogen bond and proton transfer in 2-(2′-hydroxyphenyl) benzothiazole and 2-(2′-hydroxyphenyl) benzimidazole. J Phys Chem A 102:1560–1567
39. Vollmer F, Rettig W, Birckner E (1994) Switching between charge and proton-transfer emission in the excited state of a substituted 3-hydroxyflavone. J Fluoresc 4:65–72
40. Minkin VI, Garnovskii AD, Elguero J, Katritzky AR, Denisko OV (2000) The tautomerism of heterocycles: five-membered rings with two or more heteroatoms. Adv Heterocycl Chem 76:157–323
41. Doroshenko A, Posokhov E, Verezubova A, Ptyagina L (2000) Excited state intramolecular proton transfer reaction and luminescent properties of the ortho-hydroxy derivatives of 2,5-diphenyl-1,3,4-oxadiazole. J Phys Org Chem 13:253–265
42. Padalkar VS, Tathe AB, Gupta VD, Patil VS, Phatangare KR, Sekar N (2012) Synthesis and photo-physical characteristics of ESIPT inspired 2-substituted benzimidazole, benzoxazole and benzothiazole fluorescent derivatives. J Fluoresc 22:311–322
43. Patil VS, Padalkar VS, Phatangare KR, Gupta VD, Umape PG, Sekar N (2012) Synthesis of new ESIPT-fluorescein: photophysics of pH sensitivity and fluorescence. J Phys Chem A 116:536–545
44. Padalkar VS, Gupta VD, Patil VS, Phatangare KR, Sekar N (2012) Indion 190 resin: efficient, environmentally friendly, and reusable catalyst for synthesis of benzimidazoles, benzoxazoles, and benzothiazoles. Green Chem Lett Rev 5:139–145
45. Treutler O, Ahlrichs R (1995) Efficient molecular numerical integration schemes. J Chem Phys 102:346–354
46. Becke AD (1993) A new mixing of Hartree-Fock and local density-functional theories. J Chem Phys 98:1372–1377
47. Lee C, Yang W, Parr RG (1988) Development of the Colle-Salvetti conelation energy formula into a functional of the electron density. Phys Rev B 37:785–789
48. Kim CH, Park J, Seo J, Park SJ, Joo TJ (2010) Excited state intramolecular proton transfer and charge transfer dynamics of a 2-(2′-hydroxyphenyl)benzoxazole derivative in solution. J Phys Chem A 114:5618–5629
49. Santra M, Moon H, Park MH, Lee TW, Kim Y, Ahn KH (2012) Dramatic substituent effects on the photoluminescence of boron complexes of 2-(benzothiazol-2-yl)phenols. Chem Eur J. doi:10.1002/chem.201200726
50. Li H, Niu L, Xu X, Zhang S, Gao F (2011) Excited state proton transfer in guanine in the gas phase and in water. J Fluoresc 21:1721–1728
51. Furche F, Rappaport D (2005) Density functional theory for excited states: equilibrium structure and electronic spectra. In: Olivucci M (ed) Computational photochemistry. Elsevier, Amsterdam, Vol 16, Chapter 3
52. Lakowicz JR (1999) Principles of fluorescence spectroscopy, 2nd edn. Kluwer, New York
53. Valeur B (2001) Molecular fluorescence: principles and applications. Wiley-VCH Verlag, Weinheim
54. Cossi M, Barone V, Cammi R, Tomasi J (1996) Ab initio study of solvated molecules: a new implementation of the polarizable continuum model. J Chem Phys Lett 255:327–335
55. Tomasi J, Mennucci B, Cammi R (2005) Quantum mechanical continuum solvation models. Chem Rev 105:2999–3094
56. Frisch MJ, Trucks GW, Schlegel HB, Scuseria GE, Robb MA, Cheeseman JR, Scalmani G, Barone V, Mennucci B, Petersson GA, Nakatsuji H, Caricato M, Li X, Hratchian HP, Izmaylov AF, Bloino J, Zheng G, Sonnenberg JL, Hada M, Ehara M, Toyota K, Fukuda R, Hasegawa J, Ishida M, Nakajima T, Honda Y, Kitao O, Nakai H, Vreven T, Montgomery JA Jr, Peralta JE, Ogliaro F, Bearpark M, Heyd JJ, Brothers E, Kudin KN, Staroverov VN, Kobayashi R, Normand J, Raghavachari K, Rendell A, Burant JC, Iyengar SS, Tomasi J, Cossi M, Rega N, Millam NJ, Klene M, Knox JE, Cross JB, Bakken V, Adamo C, Jaramillo J, Gomperts R, Stratmann RE, Yazyev O, Austin AJ, Cammi R, Pomelli C, Ochterski JW, Martin RL, Morokuma K, Zakrzewski VG, Voth GA, Salvador P, Dannenberg JJ, Dapprich S, Daniels AD, Farkas O, Foresman JB, Ortiz JV, Cioslowski J, Fox DJ (2010) Gaussian 09, revision C.01. Gaussian, Inc, Wallingford
57. Williams ATR, Winfield S, Miller JN (1983) Relative fluorescence quantum yields sing a computer controlled luminescence spectrometer. Analyst 108:1067–1071
58. Dhami S, De Mello AJ, Rumbles G, Bishop SM, Phillips D, Beeby A (1995) Photochem Photobiol 61:341–346
59. Reichardt C (2003) Solvent and solvent effects in organic chemistry third and enlarged edition. Wiley VCH Verlag GmbH & Co. KGaA, Weinheim